Intravoxel Incoherent Motion and Dynamic Contrast-Enhanced Magnetic Resonance Imaging to Early Detect Tissue Injury and Microcirculation Alteration in Hepatic Injury Induced by Intestinal Ischemia–Reperfusion in a Rat Model

Jiaxing Yang, MMed,[1,2] Mingzhu Meng, MMed,[1] Changjie Pan, MD,[1] Liulan Qian, MMed,[3] Yangyang Sun, MMed,[4] Haifeng Shi, MD,[1]* Yong Shen, MD,[5] and Weiqiang Dou, PhD[6]

Background: Intravoxel incoherent motion (IVIM) can provide quantitative information about water diffusion and perfusion that can be used to evaluate hepatic injury, but it has not been studied in hepatic injury induced by intestinal ischemia–reperfusion (IIR). Dynamic contrast-enhanced (DCE) magnetic resonance imaging (MRI) can provide perfusion data, but it is unclear whether it can provide useful information for assessing hepatic injury induced by IIR.
Purpose: To examine whether IVIM and DCE-MRI can detect early IIR-induced hepatic changes, and to evaluate the relationship between IVIM and DCE-derived parameters and biochemical indicators and histological scores.
Study Type: Prospective pre-clinical study.
Population: Forty-two male Sprague–Dawley rats.
Field Strength/Sequence: IVIM-diffusion-weighted imaging (DWI) using diffusion-weighted echo-planar imaging sequence and DCE-MRI using fast spoiled gradient recalled-based sequence at 3.0 T.
Assessment: All rats were randomly divided into the control group (Sham), the simple ischemia group, the ischemia–reperfusion (IR) group (IR1h, IR2h, IR3h, and IR4h) in a model of secondary hepatic injury caused by IIR, and IIR was induced by clamping the superior mesenteric artery for 60 minutes and then removing the vascular clamp. Advanced Workstation (AW) 4.6 was used to calculate the imaging parameters (apparent diffusion coefficient [ADC], true diffusion coefficient [D], perfusion-related diffusion [D^*] and volume fraction [f]) of IVIM. OmniKinetics (OK) software was used to calculate the DCE imaging parameters (K^{trans}, K_{ep}, and V_e). Alanine aminotransferase (ALT) and aspartate aminotransferase (AST) were analyzed with an automatic biochemical analyzer. Superoxide dismutase (SOD) activity was assessed using the nitro-blue tetrazolium method. Malondialdehyde (MDA) was determined by thiobarbituric acid colorimetry. Histopathology was performed with hematoxylin and eosin staining.
Statistical Tests: One-way analysis of variance (ANOVA) and Bonferroni post-hoc tests were used to analyze the imaging parameters and biochemical indicators among the different groups. Pearson correlation analysis was applied to determine the correlation between imaging parameters and biochemical indicators or histological score.
Results: ALT and MDA reached peak levels at IR4h, while SOD reached the minimum level at IR4h (all $P < 0.05$). ADC, D, D^*, and f gradually decreased as reperfusion continued, and K^{trans} and V_e gradually increased (all $P < 0.05$). The degrees of change for f and V_e were greater than those of other imaging parameters at IR1h (all $P < 0.05$). All groups showed good correlation between imaging parameters and SOD and MDA (r[ADC] = 0.615, −0.666, r[D] = 0.493, −0.612, r[D^*] = 0.607, −0.647, r[f] = 0.637, −0.682, r[K^{trans}] = −0.522, 0.500, r[V_e] = −0.590, 0.665, respectively; all $P < 0.05$). However, the IR

groups showed poor or no correlation between the imaging parameters and SOD and MDA (P [K^{trans} and MDA] = 0.050, P [D and SOD] = 0.125, P [the remaining imaging parameters] < 0.05). All groups showed a positive correlation between histological score and K^{trans} and V_e (r = 0.775, 0.874, all P < 0.05), and a negative correlation between histological score and ADC, D, f, and D^* (r = −0.739, −0.821, −0.868, −0.841, respectively; all P < 0.05). For the IR groups, there was a positive correlation between histological score and K^{trans} and V_e (r = 0.747, 0.802, all P < 0.05), and a negative correlation between histological score and ADC, D, f, and D^* (r = −0.567, −0.712, −0.715, −0.779, respectively; all P < 0.05).
Data Conclusion: The combined application of IVIM and DCE-MRI has the potential to be used as an imaging tool for monitoring IIR-induced hepatic histopathology.

Level of Evidence: 1
Technical Efficacy Stage: 2

Intestinal ischemia–reperfusion (IIR) injury is an irreversible and complex pathological process that occurs emergently in intestinal transplantation, hemorrhagic shock, intestinal volvulus, and intussusceptions.[1] IIR not only injures the viscera itself but can also affect non-ischemic distant organs. It is generally accepted that remote organs are affected by IIR as a result of inflammatory cell infiltration, reactive oxygen species (ROS), and activation of an integrated network of soluble inflammatory mediators.[2] IIR-induced hepatic injury is characterized by swelling and necrosis, and is associated with increased mortality and poor prognosis.[3] In clinical practice, diagnosis of hepatic injury is routinely based on the measurement of aspartate aminotransferase (AST) and alanine aminotransferase (ALT) in serum.[4] However, these indicators are only altered if substantial or potentially irreversible hepatic damage is present.[5]

With the rapid development of magnetic resonance imaging (MRI) techniques, functional MRI may allow early detection of the presence and severity of hepatic abnormalities.[6] Previous studies have shown that pure water diffusion and blood perfusion can be separated by using the intravoxel incoherent motion (IVIM) technique, which is a biexponential model fitted to low b-value diffusion-weighted imaging (DWI) data.[7,8] The IVIM model can be used to calculate the apparent diffusion coefficient (ADC), the true diffusion coefficient (D), the perfusion-related diffusion (D^*), and the volume fraction (f). Therefore, IVIM may provide important information to detect microcirculation and hepatic fluid loading, which makes it particularly appealing for quantifying early hepatic injury.[6] Based on pharmacokinetic models, the hemodynamic parameters of dynamic contrast-enhanced (DCE)-MRI can be a valuable aid in the diagnosis and measurement of tissue perfusion and vascular permeability.[9–11] Although the volume transfer constant (K^{trans}), rate constant (K_{ep}), and volume of extravascular extracellular space (EES) per unit volume of tissue (V_e) were confirmed to detect blood–brain barrier disruption, there was little application to understand liver injury evoked by IIR.[12]

Thus, the aim of this study was to elevate the situation of hepatic pathophysiological alterations using IVIM and DCE-MRI in rat model, and to explore the correlation between image parameters and the degree of liver damage.

Materials and Methods

Animals

Forty-two male Sprague–Dawley (SD) rats weighing 200–250 g were acquired from the animal experiment center. The rats were randomly divided into six groups: treated with ischemic reperfusion lasting 1 hour (IR1h), ischemic reperfusion lasting 2 hours (IR2h), ischemic reperfusion lasting 3 hours (IR3h), ischemic reperfusion lasting 4 hours (IR4h), a control group (Sham), and a group treated with simple ischemic treatment lasting 1 hour (I1h) (N = 7 rats per group). They were placed on a homoeothermic cushion to maintain body temperature. The rats were fasted from food for 12 hours before the operation. Surgery was performed under anesthesia, which was induced by injecting 5% chloral hydrate via the abdomen. IIR was induced by clamping the superior mesenteric artery for 60 minutes with a nontraumatic vascular clamp and then removing the vascular clamp for 1 hour, 2 hours, 3 hours, or 4 hours, or by only tightening the superior mesenteric artery for 1 hour using the surgical suture according to the method outlined by Kim et al.[13] The control group underwent laparotomy and mesentery dissection only.

Magnetic Resonance Imaging Protocol

All examinations were performed using a 3 T scanner (Discovery 750 W, GE Healthcare, USA) with a surface soft coil (GE Healthcare, USA). To minimize the respiration motion artifact, in addition to the application of anesthesia, an abdominal belt was used for each rat in the MRI experiment. With these procedures, the breath patterns of all experimental rats were consistent during the experiment. Each rat was placed in the scanner head first and supine.

The imaging protocol comprised axial T_2-weighted fast spin echo (FSE) images (2D, repetition time [TR]/echo time [TE] = 5536/56 msec, slice thickness = 2 mm, field of view [FOV] = 80 × 80 mm^2, matrix = 160 × 160), coronal T_1-weighted FSE images (TR/TE = 8.9/1.1 msec, slice thickness = 2 mm, FOV = 90 × 55 mm^2, matrix = 160 × 160), coronal T_2-weighted FSE images (TR/TE = 3572/71 msec, slice thickness = 2 mm, FOV = 90 × 55 mm^2, matrix = 160 × 160), axial IVIM DWI (TR/TE = 3183/76 msec, slice thickness = 2 mm, FOV = 80 × 80 mm^2, matrix = 160 × 160, 9 b-values = 20, 40, 60, 80, 100, 150, 200, 500, and 800 s/mm^2 acceleration factor [array spatial sensitivity encoding technique] = 2) and coronal DCE (fast spoiled gradient recalled based sequence, TR/TE = 8.9/1.2 msec, slice thickness = 2 mm, acceleration factor = 2, FA = 12°, FOV = 90 × 55 mm^2, matrix = 160 × 160, the time resolution was 8 s for a total of 45 time points).
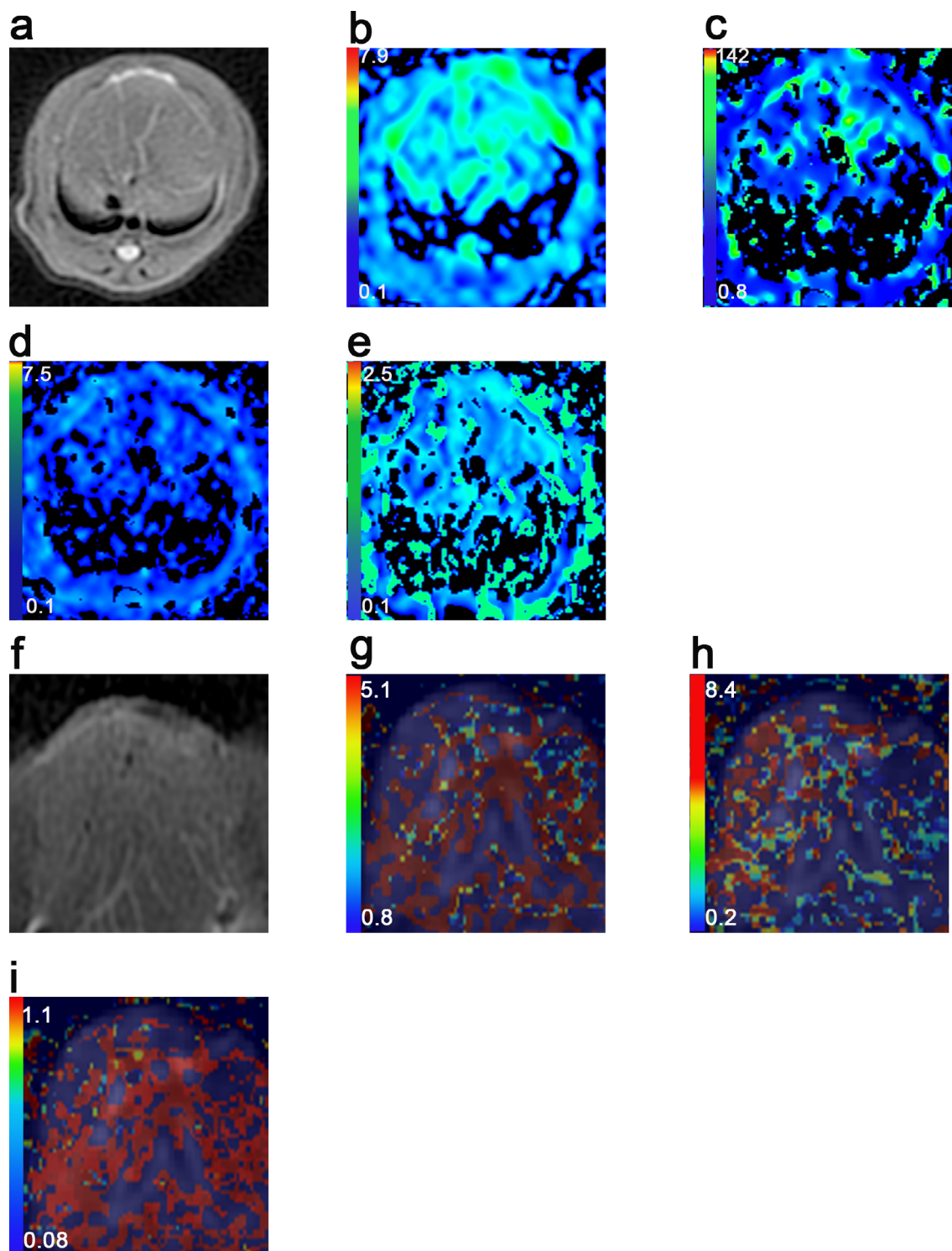
FIGURE 1: Demonstration of intravoxel incoherent motion (IVIM) and dynamic contrast-enhanced (DCE) magnetic resonance imaging. (a) Axial T$_2$WI image of the liver. (b) Corresponding ADC map from monoexponential fitting with 9 b-values. (c–e) Parametric maps of IVIM (D^*, D, and f) from biexponential fitting with 9 b-values. (f) Coronal T$_2$WI image of the liver. (g–i) Parametric maps of DCE obtained from improved the Tofts–Kermode two-compartment model.

Intravoxel Incoherent Motion Diffusion-Weighted MRI Analysis

IVIM-DWI data were processed by using Advanced Workstation (AW 4.6) (GE Healthcare). The nonlinear least-squares curve fittings by means of the Levenberg–Marquardt method were performed using a biexponential model of 9 b-values to acquire the D, D^*, and f values according to the following equation:

$$S_b/S_0 = (1-f) \cdot \exp(-b \cdot D) + f \cdot \exp(-b \cdot D^*). \quad (1)$$

S_0 represents the signal intensity at the b-value of 0, and S_b expressed signal intensity at the specific b-value. D represents the true diffusion as reflected by pure water-molecular diffusion. D^* represents the pseudo-diffusion related to perfusion. f represents the perfusion fraction reflected as a fractional volume of microcirculation within a voxel.

The ADC value was calculated by the monoexponential model, using the following equation:

$$S_b/S_0 = \exp\left(-b\text{ADC}\right). \quad (2)$$

Dynamic Contrast-Enhanced MRI Analysis

DCE-MRI data were imported into OmniKinetics (OK) software for processing (GE Pharmaceutical). Three quantitative pharmacokinetic DCE-MRI parameters (K^{trans}, K_{ep}, and V_e) were acquired using the improved Tofts–Kermode two-compartment model (Fig. 1).

TABLE 1. Intraobserver and Interobserver Agreement in Measurements

	Intraobserver	Interobserver
ADC	0.930[a] (0.910–0.945)	0.959[a] (0.947–0.968)
D	0.969[a] (0.960–0.976)	0.945[a] (0.931–0.957)
D^*	0.973[a] (0.965–0.979)	0.924[a] (0.904–0.940)
f	0.941[a] (0.924–0.954)	0.927[a] (0.907–0.943)
K^{trans}	0.949[a] (0.935–0.960)	0.912[a] (0.888–0.930)
K_{ep}	0.842[a] (0.801–0.874)	0.805[a] (0.739–0.853)
V_e	0.968[a] (0.959–0.975)	0.938[a] (0.921–0.951)

[a]Excellent agreement with intraclass correlation coefficient >0.75.

Region of Interest Analysis

First, motion artifacts and soft tissue resolution of the obtained images were subjectively evaluated by three radiologists (C.J.P., M.Z.M., and H.F.S.). Once distinct or severe motion artifacts were found and unanimously confirmed by three people, the images were removed. Soft tissue resolution could distinguish the liver boundary and the main vessels unanimously confirmed by the three investigators. Subsequently, all regions of interest (ROI) in the right lobe of the liver were manually drawn by two radiologists (J.X.Y. and M.Z.M., with 3 and 8 years of experience in abdominal imaging, respectively) on axial or coronal T_2-weighted images (T_2WI), and were then duplicated to the corresponding ADC, D^*, D, f, K_{trans}, K_{ep}, and V_e. After selecting two central slices of each liver, three circular ROIs were manually drawn per slice to avoid including hepatic duct, large hepatic vessels, and inhomogeneous areas. All ROIs in the liver were manually drawn with a size of 6–8 mm^2, and the mean value of the six ROIs was calculated for the final analysis. The ROI-specific IVIM and DCE-derived parameter values (ADC, D, D^*, f, K^{trans}, and V_e) were obtained for each animal. The mean values of parameters in the Sham group were considered as the baseline and were used to scale the corresponding mean values of the I1h, IR1h, IR2h, IR3h, and IR4h groups. The resultant ratios were used for further data analysis.

Biochemical Assessment and Histological Analysis

This prospective study was approved by the Institutional Review Board of Changzhou Second People's Hospital. After MRI scanning, 6 mL blood was collected from the inferior vena cava of the rats to obtain serum. The levels of ALT and AST were measured by an automatic biochemical analyzer (Cobas 8000, Roche). The rats were killed to collect the left lateral lobe of liver to assess malondialdehyde (MDA) and superoxide dismutase (SOD). SOD activity was assayed using the nitro-blue tetrazolium method, as previously described by Sun et al.[14] MDA was determined by thiobarbituric acid colorimetry, as previously described by Wong et al.[15]

The right lobe of liver was obtained after sacrifice for histological examination. The samples were immediately fixed in 5% buffered

TABLE 2. Biochemical Indicators at Different Time Points During the Progression of Hepatic Injury

	N (42)	AST (U/liter)	ALT (U/liter)	MDA (nmol/mg)	SOD (U/mg)
Sham	7	160 ± 49	62.5 ± 12.8	0.59 ± 0.08	367 ± 19
I1h	7	158 ± 43	111 ± 36	0.67 ± 0.07	330 ± 23
IR1h	7	184 ± 56	92.5 ± 45.4	0.70 ± 0.05[*]	323 ± 10[*]
IR2h	7	184 ± 55	110 ± 23	0.77 ± 0.06[*]	310 ± 32[*]
IR3h	7	190 ± 42	98.2 ± 30.0	0.77 ± 0.05[*]	319 ± 10[*]
IR4h	7	204 ± 68	141 ± 29[*]	0.80 ± 0.09[*]	290 ± 39[*]
F		0.787	4.834	10.220	7.358
P		0.566	0.002	<0.05	<0.05

[*]$P < 0.05$ indicates statistical significance compared to the Sham group.

TABLE 3. Intravoxel Incoherent Motion (IVIM) and Dynamic Contrast-Enhanced (DCE) Parameters at Different Time Points During the Progression of Hepatic Injury

	N (42)	ADC	D	D*	f	K^trans	K_ep	V_e
Sham	7	1.70 ± 0.28	1.63 ± 0.20	111 ± 15	40.8 ± 1.4	1.53 ± 0.27	4.62 ± 0.33	0.26 ± 0.03
I1h	7	1.68 ± 0.28	1.62 ± 0.22	108 ± 23	39.9 ± 2.1	1.54 ± 0.32	4.60 ± 0.33	0.27 ± 0.03
IR1h	7	1.59 ± 0.23	1.56 ± 0.24	105 ± 14	$36.9 \pm 2.0^*$	1.61 ± 0.26	4.59 ± 0.28	$0.31 \pm 0.03^*$
IR2h	7	$1.51 \pm 0.23^*$	$1.45 \pm 0.24^*$	$86.7 \pm 14.5^*$	$35.2 \pm 1.5^*$	$1.80 \pm 0.25^*$	4.56 ± 0.28	$0.44 \pm 0.03^*$
IR3h	7	$1.43 \pm 0.23^*$	$1.34 \pm 0.16^*$	$72.8 \pm 13.4^*$	$32.3 \pm 1.3^*$	$1.93 \pm 0.22^*$	4.52 ± 0.28	$0.52 \pm 0.04^*$
IR4h	7	$1.32 \pm 0.21^*$	$1.12 \pm 0.14^*$	$53.7 \pm 10.6^*$	$30.3 \pm 2.3^*$	$3.36 \pm 0.29^*$	4.54 ± 0.28	$0.71 \pm 0.03^*$
F		15.688	38.613	92.470	224.663	290.881	0.680	1365.890
P		<0.05	<0.05	<0.05	<0.05	<0.05	0.639	<0.05

*$P < 0.05$ indicates statistical significance compared to the Sham group.
Values of ADC, D, D^*, f, K^{trans}, K_{ep}, and V_e expressed as means $\pm$ SDs, and compared with one-way analysis of variance and Bonferroni post-hoc test. The mean ADC, D, and D^* are expressed in $\times 10^{-3}$ mm^2/s, and f is expressed in %.

formalin, embedded in paraffin, and then cut into sections of 5 μm thickness. Hematoxylin and eosin (H&E) staining was performed on each section for histological assessment. Hepatic injury was scored according to Eckhoff et al.[16] Grade 0, normal liver tissue; Grade 1, mild injury, partial hepatocyte degeneration (swelling and steatosis); Grade 2, moderate injury, extensive hepatocellular degeneration with partial hepatocellular necrosis; Grade 3, severe injury, hepatocyte necrosis, absence or ambiguity of hepatic cord structure with bleeding and neutrophils infiltration. All assessments were performed by a histopathologist with 10 years of experience in hepatic pathology (Y.Y. S.), who was blinded to the identity of the animal group.

Statistical Analyses

All statistical analyses were performed with SPSS 24.0 (Chicago, IL, USA) and GraphPad Prism 5.0 (San Diego, CA, USA). The intraclass correlation coefficient (ICC) was used to determine the intraobserver and interobserver agreement of IVIM and DCE parameters, with ICC <0.40, 0.40–0.75, >0.75 indicating poor, fair to good, and excellent agreement, respectively.[17] One-way analysis of variance (ANOVA) and Bonferroni post-hoc tests were used to test the differences in imaging parameters and biochemical indicators among groups. Pearson correlation analysis was applied to determine the correlation between imaging parameters and biochemical indicators and histological score. P-values <0.05 indicated statistical significance.

Results

Intraobserver and Interobserver Agreement of IVIM and DCE Parameters

The ICCs of IVIM and DCE parameters are summarized in Table 1.

Biochemical Indicators at Different Time Points

ALT and MDA reached peak levels at IR4h, and SOD reached the minimum level at IR4h (all $P < 0.05$). There was no significant difference for AST in any of the groups ($P = 0.566$) in Table 2.

IVIM and DCE Parameters at Different Time Points

ADC, D, f, and D^* showed progressive reduction as reperfusion continued (all $P < 0.05$), and K^{trans} and V_e gradually increased (all $P < 0.05$) (Table 3). At 2 hours (IR1h), the f and V_e values showed a different trend compared to the other imaging parameters in that they decreased and increased by 9.70% ($P < 0.05$) and 22.61% ($P < 0.05$), respectively (Fig. 2a,b).

Correlation between Imaging Parameters and Biochemical Indicators

The results in Table 4 indicate that MDA was negatively correlated with ADC, D, D^*, and f ($r = -0.666$, -0.612, -0.647, -0.682, all $P < 0.05$), and positively correlated with K^{trans} and V_e ($r = 0.500$ and 0.665, all $P < 0.05$) in all groups. Meanwhile, SOD was positively correlated with ADC, D, D^*, and f ($r = 0.615$, 0.493, 0.607, 0.637, all
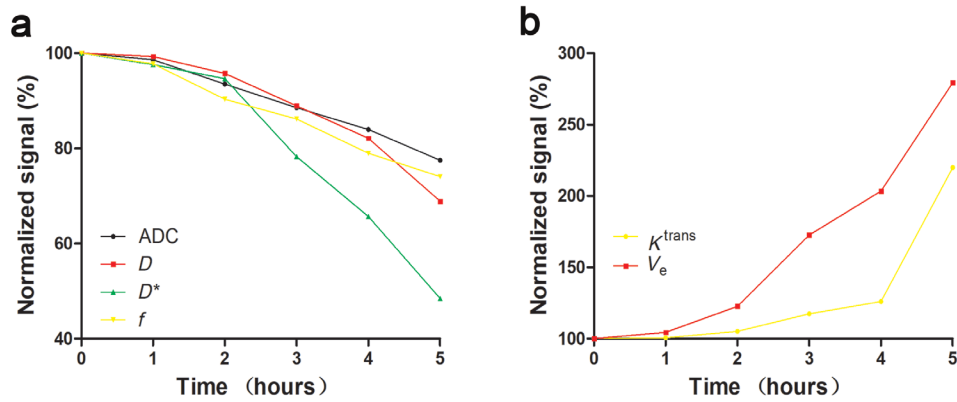
FIGURE 2: Changes in tissue diffusion and perfusion studied by intravoxel incoherent motion (IVIM) and dynamic contrast-enhanced (DCE) parameters. (a) The relative change in ADC (black line), D (red line), D^* (green line), and f (yellow line) at sham, 1 hour (I1h), 2 hours (IR1h), 3 hours (IR2h), 4 hours (IR3h), and 5 hours (IR4h). (b) The relative change in K^{trans} (yellow line) and V_e (red line) at sham, 1 hour (I1h), 2 hours (IR1h), 3 hours (IR2h), 4 hours (IR3h), and 5 hours (IR4h).

TABLE 4. Correlation Between Intravoxel Incoherent Motion (IVIM) and Dynamic Contrast-Enhanced (DCE) Parameters and Biochemical Indicators

	Inclusion of all groups				Inclusion of only ischemia–reperfusion groups			
	MDA (nmol/mg)		SOD (U/mg)		MDA (nmol/mg)		SOD (U/mg)	
Parameters	Correlation coefficient	P-value	Correlation coefficient	P-value	Correlation coefficient	P-value	Correlation coefficient	P-value
ADC	−0.666	<0.05	0.615	<0.05	−0.379	0.047	0.441	0.019
D	−0.612	<0.05	0.493	0.001	−0.446	0.017	0.297	0.125
D^*	−0.647	<0.05	0.607	<0.05	−0.489	0.008	0.441	0.019
f	−0.682	<0.05	0.637	<0.05	−0.405	0.032	0.417	0.027
K^{trans}	0.500	0.001	−0.522	<0.05	0.374	0.050	−0.455	0.015
V_e	0.665	<0.05	−0.590	<0.05	0.492	0.001	−0.422	0.025

P-value <0.05 indicates statistical significance.

$P < 0.05$), and negatively correlated with K^{trans} and V_e value ($r = -0.522$ and -0.590, all $P < 0.05$) in all groups. Compared to all groups, the correlation between imaging parameters and MDA and SOD significantly decreased in the ischemia–reperfusion (IR) groups (r [ADC] $= -0.379$, 0.441, all $P < 0.05$; r [D] $= -0.446$ [$P < 0.05$], 0.297 [$P = 0.125$]; r [D^*] $= -0.489$, 0.441, all $P < 0.05$; r [f] $= -0.405$, 0.417, all $P < 0.05$; r [K^{trans}] $= 0.374$ [$P = 0.050$], -0.455 [$P < 0.05$]; r [V_e] $= 0.492$, -0.422, all $P < 0.05$).

Correlation between Imaging Parameters and Histological Score

In all groups, there was a positive correlation between histological score and K^{trans} and V_e ($r = 0.775, 0.874$), and there was a negative correlation between histological score and ADC, D, f, and D^* ($r = -0.739, -0.821, -0.868, -0.841$, respectively; all $P < 0.05$) (Fig. 3). In the IR groups, there was a positive
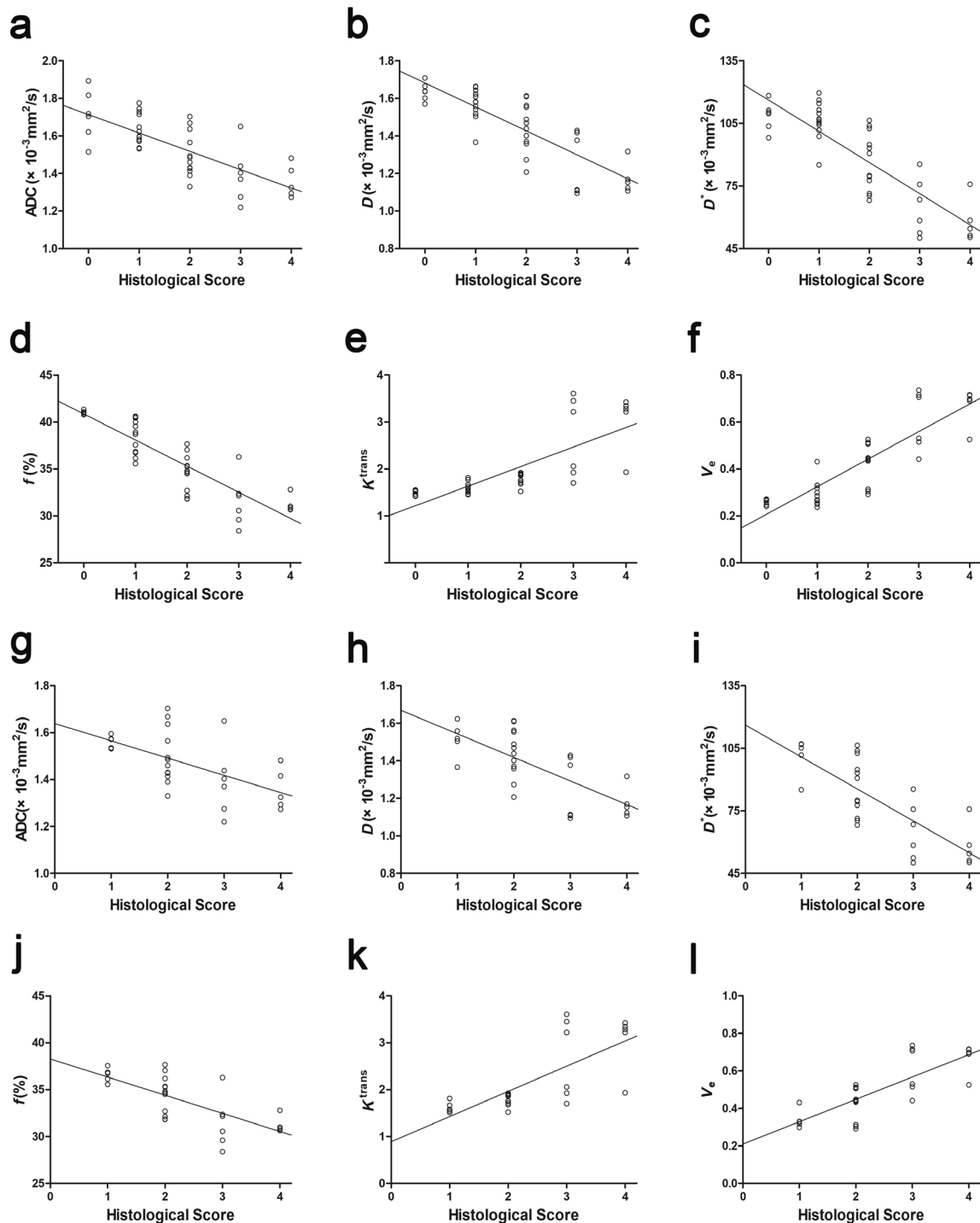
correlation between histological score and K^{trans} and V_e ($r = 0.747, 0.802$), and there was a negative correlation between histological score and ADC, D, f, and D^* value ($r = -0.567, -0.712, -0.715, -0.779$, all $P < 0.05$) (Fig. 3).

Pathological Progress of IIR-Induced Hepatic Injury

The H&E staining showed a clear progressive change in the hepatic structure in Fig. 4.

Discussion

Recent advances have shown that IVIM promoted the application for evaluating hepatic fibrosis using quantitative parameters.[18] Relevant DCE-MRI parameters contribute to identification of the degree of malignancy of gliomas.[10] IVIM and DCE-MRI may be used as noninvasive methods to assess changes in diffusion, perfusion, vascular permeability, and microcirculation.

FIGURE 3: Changes in diffusion and perfusion in tissue studied by corresponding parameters in intravoxel incoherent motion (IVIM) and dynamic contrast-enhanced (DCE) magnetic resonance imaging. (a–f) Scatter plots showing the correlations between histological score and ADC value ($r = -0.739$, $P < 0.001$), D value ($r = -0.821$, $P < 0.001$), D^* value ($r = -0.841$, $P < 0.001$), f value ($r = -0.868$, $P < 0.001$), K^{trans} value ($r = 0.775$, $P < 0.001$), and V_e value ($r = 0.874$, $P < 0.001$) for all groups. (j–l) Scatter plots showing the correlation between histological score and ADC value ($r = -0.567$, $P < 0.001$), D value ($r = -0.712$, $P < 0.001$), D^* value ($r = -0.779$, $P < 0.001$), f value ($r = -0.715$, $P < 0.001$), K^{trans} value ($r = 0.747$, $P < 0.001$), and V_e value ($r = 0.802$, $P < 0.001$) for ischemia–reperfusion groups.

In this study, compared with the Sham group, ALT was significantly elevated in the IR4h group, and there was no significant difference in AST in any of the groups, which may indicate that AST and ALT are insufficiently sensitive to early IIR-induced liver injury. These data showed that MDA reached the peak level at IR4h, and SOD reached the minimum level at IR4h, indicating that oxidative stress occurs during IIR.
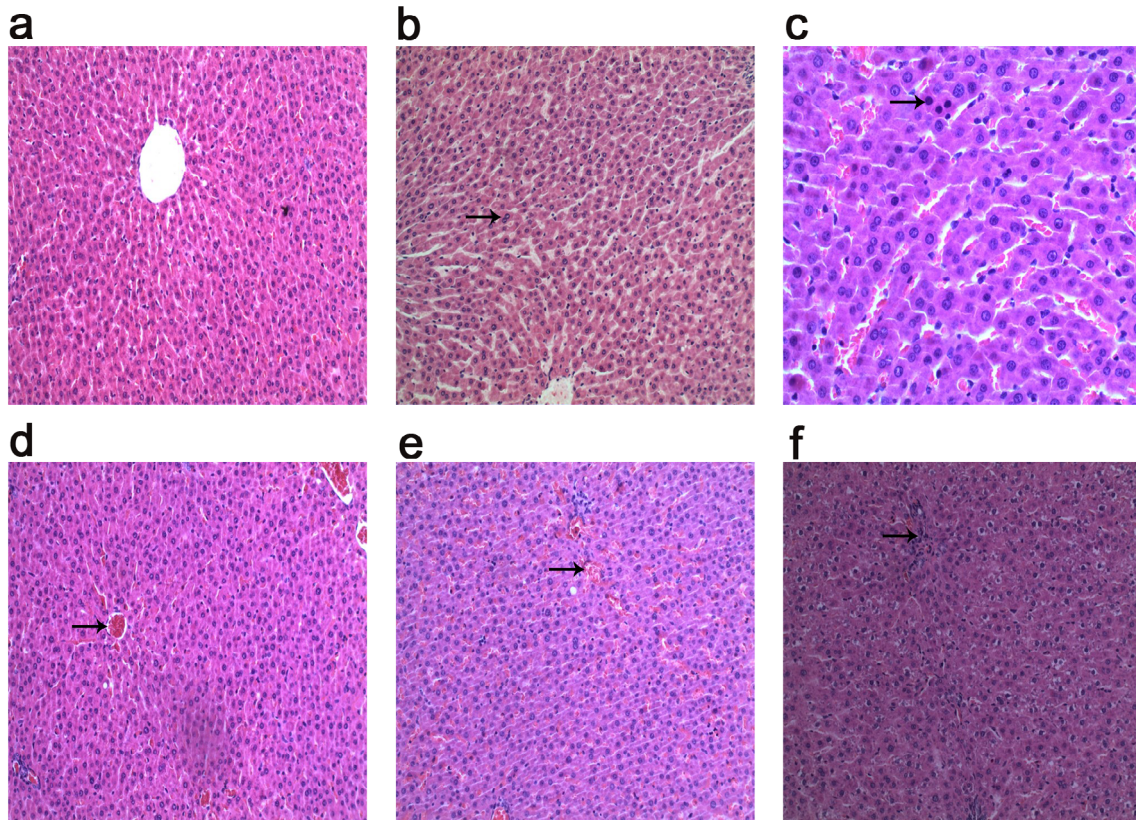
FIGURE 4: Representative histological liver sections (H&E stain; magnification, ×200) at different time points during the course of IIR. (a) Normal liver structure in the Sham group. **(b)** In the I1h group, a small number of proliferating hepatocytes can be observed. **(c)** In the IR1h group, pyknosis is apparent in some hepatocytes. **(d)** In the IR2h group, hyperemia was observed in the hepatic sinus with surrounding cloudy and swollen hepatocytes. **(e)** In the IR3h group, the number of hepatocytes with pyknosis increased significantly, and congestion was obvious in the hepatic tissues. **(f)** In the IR4h group, significant degeneration and necrosis of hepatocytes is observed, in addition to disappearance of the hepatic boundary plate and destruction of the sinus cord structure.

Furthermore, there were no significant differences in IVIM and DCE-MRI parameters in the I1h group compared with the Sham group, which implies that IIR rather than simple intestinal ischemia evoked secondary hepatic injury. The data showed that ADC and D gradually decreased from the Sham group to the IR4h group. These results indicate that IIR can promote a progressive reduction in intrahepatic diffusion, which might be due to swollen hepatic cells, as confirmed in the H&E examinations at the corresponding time points.[19] IIR might cause a release of inflammatory cytokines, leukocytes, and chemokines, which can lead to "sodium pump" inactivation for the net gain of water in the hepatocytes.[20,21] In accordance with a previous study[22] that showed that the values of f and D^* reduced with the aggravation of hepatic injury, this study also showed that the values f and D^* gradually decreased from the Sham group to the IR4h group, which indicated that these findings demonstrate a decreased blood volume and the presence of microcirculatory disorder in the liver. The H&E examinations showed that both hepatic sinusoid congestion blocking intrahepatic vessels and hepatocyte edema degeneration compressing intrahepatic vessels caused the changes in f and D^*.[3,23]

Moreover, the data showed that the K^{trans} value gradually increased from the Sham group to the IR4h group. An Increased K^{trans} implies the increase in vascular permeability, related to vascular endothelial cell injury by inflammatory cytokines, activated Kupffer cells, increased ROS, and reduced nitric oxide (NO).[3,24–26] This study showed that the V_e value gradually increased from the Sham group to the IR4h group, indicating an expansion of the EES volume. This phenomenon is considered to be mainly related to hepatocellular necrosis and vacuolization, as demonstrated by H&E examinations.[27–29] This study showed that the degrees of change in f and V_e were higher than those of other imaging parameters at 2 hours (IR1h), which implied that perfusion plays a more important role in early hepatic injury induced by IIR. Regrettably, in the present study, the K_{ep} value did not reduce significantly with prolonged reperfusion time, although it did show a declining tendency. This lack of significance is likely due to an insufficient reperfusion time and minor sample size.

The data also revealed that MDA was negatively correlated with ADC, D, D^*, and f, and positively correlated with K^{trans} and V_e value in all groups. Meanwhile, SOD was

positively correlated with ADC, D, D^*, and f, and negatively correlated with K^{trans} or V_e in all groups. However, the correlation between imaging parameters and MDA and SOD was poor for the IR groups. The change in imaging parameters suggests the existence of cellular oxidative stress injury, but it has limited ability to demonstrate the tendency for variations of these parameters during reperfusion. Moreover, there was a significantly positive correlation between histological score and K^{trans} and V_e, and a significantly negative correlation between histological score and ADC, D, f, and D^* in all groups and only IR groups, which probably contributed to assessing the degree of damage in hepatic parenchyma. Furthermore, the correlation between D^* and histological score was higher than that between ADC and D and histological score, which implied that compared with the diffusion parameters, the perfusion parameters are more sensitive to IIR-induced hepatic injury, which are crucial factors for evaluating hepatic dysfunction.[24,30]

Limitations

This study has several limitations. First, while selecting the ROI, we only measured the right lobe of the liver in order to maintain consistency with the pathological samples and reduce heartbeat artifacts. However, this method might fail to reflect the overall liver damage. Second, the sample size was small, and the reperfusion time was short. Thus, it was difficult to observe overall changes of hepatic injury and biochemical indicators, mainly due to the higher mortality rate of rats with a prolonged intestinal reperfusion time.

Conclusion

This study demonstrated that IVIM and DCE-MRI can non-invasively estimate hepatic pathophysiological processes in a rat IIR-induced hepatic injury model. The change in microcirculation and perfusion seemed to be the major factors in IIR-induced hepatic injury. Third, f, D^*, and V_e were more sensitive for histological change, which implies that IVIM and DCE-MRI might provide effective parameters in the process of IIR-induced hepatic injury.

Acknowledgments

References

1. Zhao W, Gan X, Su G, et al. The interaction between oxidative stress and mast cell activation plays a role in acute lung injuries induced by intestinal ischemia-reperfusion. J Surg Res 2014;187:542-552.

2. Voisin MB, Leoni G, Woodfin A, et al. Neutrophil elastase plays a non-redundant role in remodeling the venular basement membrane and neutrophil diapedesis post-ischemia/reperfusion injury. J Pathol 2019; 248:88-102.

3. Eltzschig HK, Eckle T. Ischemia and reperfusion—from mechanism to translation. Nat Med 2011;17:1391-1401.

4. Yu YM, Ni QQ, Wang ZJ, Chen ML, Zhang LJ. Multiparametric functional magnetic resonance imaging for evaluating renal allograft injury. Korean J Radiol 2019;20:894-908.

5. Privratsky JR, Wang N, Qi Y, et al. Dynamic contrast-enhanced MRI promotes early detection of toxin-induced acute kidney injury. Am J Physiol Renal Physiol 2019;316:351-359.

6. Ye W, Li J, Guo C, et al. Can intravoxel incoherent motion diffusion-weighted imaging characterize the cellular injury and microcirculation alteration in hepatic ischemia-reperfusion injury? An animal study. J Magn Reson Imaging 2016;43:1327-1336.

7. Wei Y, Gao F, Wang M, et al. Intravoxel incoherent motion diffusion-weighted imaging for assessment of histologic grade of hepatocellular carcinoma: Comparison of three methods for positioning region of interest. Eur Radiol 2019;29:535-544.

8. Mürtz P, Sprinkart AM, Reick M, et al. Accurate IVIM model-based liver lesion characterisation can be achieved with only three b-value DWI. Eur Radiol 2018;28:4418-4428.

9. Zhang N, Zhang L, Qiu B, Meng L, Wang X, Hou BL. Correlation of volume transfer coefficient Ktrans with histopathologic grades of gliomas. J Magn Reson Imaging 2012;36:355-363.

10. Haroon HA, Buckley DL, Patankar TA, et al. A comparison of Ktrans measurements obtained with conventional and first pass pharmacokinetic models in human gliomas. J Magn Reson Imaging 2004;19: 527-536.

11. Kim YS, Kim M, Choi SH, et al. Altered vascular permeability in migraine-associated brain regions: Evaluation with dynamic contrast-enhanced MRI. Radiology 2019;292:713-720.

12. Pickup S, Chawla S, Poptani H. Quantitative estimation of dynamic contrast enhanced MRI parameters in rat brain gliomas using a dual surface coil system. Acad Radiol 2009;16:341-350.

13. Kim K, Li Y, Jin G, et al. Effect of valproic acid on acute lung injury in a rodent model of intestinal ischemia reperfusion. Resuscitation 2012;83: 243-248.

14. Sun Y, Oberley LW, Li Y. A simple method for clinical assay of superoxide dismutase. Clin Chem 1988;34:497-500.

15. Wong SH, Knight JA, Hopfer SM, Zaharia O, Leach CN, Sunderman FW. Lipoperoxides in plasma as measured by liquid-chromatographic separation of malondialdehyde-thiobarbituric acid adduct. Clin Chem 1987;33:214-220.

16. Eckhoff DE, Bilbao G, Frenette L, Thompson JA, Contreras JL. 17-Beta-estradiol protects the liver against warm ischemia/reperfusion injury and is associated with increased serum nitric oxide and decreased tumor necrosis factor-alpha. Surgery 2002;132:302-309.

17. Kang KM, Lee JM, Yoon JH, Kiefer B, Han JK, Choi BI. Intravoxel incoherent motion diffusion-weighted MR imaging for characterization of focal pancreatic lesions. Radiology 2014;270:444-453.

18. Wu CH, Ho MC, Jeng YM, et al. Assessing hepatic fibrosis: Comparing the intravoxel incoherent motion in MRI with acoustic radiation force impulse imaging in US. Eur Radiol 2015;25:3552-3559.

19. Harada N, Okajima K, Uchiba M. Dalteparin, a low molecular weight heparin, attenuates inflammatory responses and reduces ischemia-reperfusion-induced liver injury in rats. Crit Care Med 2006;34:1883-1891.

20. Han SJ, Li H, Kim M, D'Agati V, Lee HT. Intestinal toll-like receptor 9 deficiency leads to paneth cell hyperplasia and exacerbates kidney, intestine, and liver injury after ischemia/reperfusion injury. Kidney Int 2019;95:859-879.

21. Du J, Fan X, Yang B, et al. Irisin pretreatment ameliorates intestinal ischemia/reperfusion injury in mice through activation of the Nrf2 pathway. Int Immunopharmacol 2019;73:225-235.

22. Li J, Jiang J, Chu Z, et al. Multiparametric MRI evaluation of liposomal prostaglandins E1 intervention on hepatic warm ischemia-reperfusion injury in rabbits. J Magn Reson Imaging 2020;52:217-228.

23. Kato H, Hamada T, Kuriyama N, et al. Role of spleen in hepatic ischemia reperfusion injury: Splenic congestion during ischemia accelerates leukocyte infiltration within the liver after reperfusion. Hepatol Res 2017;47:132-141.

24. Horie Y, Ishii H. Liver dysfunction elicited by gut ischemia–reperfusion. Pathophysiology 2001;8:11-20.

25. Park SW, Kim M, Kim JY, et al. Paneth cell-mediated multiorgan dysfunction after acute kidney injury. J Immunol 2012;189:5421-5433.

26. Kageyama S, Hata K, Tanaka H, et al. Intestinal ischemic preconditioning ameliorates hepatic ischemia/reperfusion injury in rats: Role of heme oxygenase 1 in the second window of protection. Liver Transpl 2015;21:112-122.

27. Jain R. Measurements of tumor vascular leakiness using DCE in brain tumors: Clinical applications. NMR Biomed 2013;26:1042-1049.

28. Aref M, Chaudhari AR, Bailey KL, Aref S, Wiener EC. Comparison of tumor histology to dynamic contrast enhanced magnetic resonance imaging-based physiological estimates. Magn Reson Imaging 2008;26: 1279-1293.

29. Zakhari N, Taccone MS, Torres CH, et al. Prospective comparative diagnostic accuracy evaluation of dynamic contrast-enhanced (DCE) vs. dynamic susceptibility contrast (DSC) MR perfusion in differentiating tumor recurrence from radiation necrosis in treated high-grade gliomas. J Magn Reson Imaging 2019;50:573-582.

30. Sun J, Wu Q, Sun H, Qiao Y. Inhibition of histone deacetylase by butyrate protects rat liver from ischemic reperfusion injury. Int J Mol Sci 2014;15:21069-21079.